Proceedings IRG Annual Meeting (ISSN 2000-8953)

IRG/WP 14-40674

THE INTERNATIONAL RESEARCH GROUP ON WOOD PROTECTION

Section 4 **Processes and properties**

Modern Instrumental Methods to Investigate the Mechanism of Biological Decay in Wood Plastic Composites

Grace Sun[1], Rebecca Ibach[2], Marek Gnatowski[1], Jessie Glaeser[3], Mathew Leung[1], and John Haight[3]

[1]Polymer Engineering Company
110-3070 Norland Avenue
Burnaby, British Columbia, V5B 3A6, Canada

[2]USDA Forest Service
Forest Products Laboratory
One Gifford Pinchot Drive
Madison, Wisconsin, 53726 USA

[3] USDA Forest Service
Northern Research Station, Center for Forest Mycology Research
One Gifford Pinchot Drive
Madison, Wisconsin, 53726 USA

Paper prepared for the 45th IRG Annual Meeting
St George, Utah, USA
11-15 May 2014

IRG SECRETARIAT
Box 5609
SE-114 86 Stockholm
Sweden
www.irg-wp.com

Modern Instrumental Methods to Investigate the Mechanism of Biological Decay in Wood Plastic Composites

Grace Sun[1], Rebecca Ibach[2], Marek Gnatowski[1], Jessie Glaeser[3], Mathew Leung[1], John Haight[3]

[1] Polymer Engineering Company, 110-3070 Norland Avenue, Burnaby, BC, Canada V5B 3A6, grace.sun@polymerengineering.ca

[2] USDA Forest Service Forest Products Laboratory, One Gifford Pinchot Drive, Madison, WI, USA 53726

[3] USDA Forest Service, Northern Research Station, Center for Forest Mycology Research, One Gifford Pinchot Dr., Madison, WI, USA 53726

ABSTRACT

Various instrumental techniques were used to study the fungal decay process in wood plastic composite (WPC) boards. Commercial boards exposed near Hilo, Hawaii (HI) for eight years in both sun and shadow locations were inspected and tested periodically. After eight years of exposure, both boards were evaluated using magnetic resonance imaging (MRI), while a selected area of the board exposed in shadow was additionally tested using microscopy and micro x-ray computed tomography (CT). Experimental boards exposed to either exterior conditions in Vancouver, British Columbia (BC) or a laboratory decay process were used for verification of MRI and CT results obtained from the commercial board. MRI detected the presence of free water and its distribution in the exposed commercial board samples tested. Fibre saturation in the experimental board was found to be about 22%, in comparison to 27 – 30% present in most wood species. There was good correlation between the detection of free water by MRI and by destructive testing. Reconstructed volumes from CT scans of the tested boards allowed for the WPC microstructure to be observed in various planes of view and for void analysis of the material to be conducted. A significantly higher average percentage volume of voids was detected in the exposed sample compared to its reference unexposed counterpart. CT scans and subsequent void analysis of the experimental soil block culture test samples of known weight loss in wood demonstrated this technique to be reasonably accurate in the detection of voids created due to biological decay. No obvious relationship was established between the presence of free water detected by MRI and the average volume of voids detected by CT. Scanning electron microscopy (SEM) confirmed the presence of fungal mycelia in the exposed commercial board cross-section imaged by both MRI and CT. It was confirmed that both MRI and micro CT could be used for non-destructive evaluations of WPC materials, including their decay process. This work also found that many different decay fungi species could colonize and internally damage WPC, and that fungal decay in WPC seems to be a self-propagating process requiring an initiation time period where no obvious decay damage is observed.

Keywords: computed tomography, exterior exposure, magnetic resonance imaging, microstructure, moisture content, scanning electron microscopy, soil block culture test, water absorption, wood plastic composite, void analysis

1. INTRODUCTION

There is limited and controversial knowledge within industry and academia related to the mechanism of decay in wood plastic composite (WPC) materials. WPC's are used for many applications, and a large portion (about two-thirds) are used for outdoor construction such as decking, railings, and fencing, as well as exterior cover applications such as siding and trim. These new WPC products are expected to be designed for long-term performance, consistent appearance, and dimensional stability (Smith and Wolcott 2006). WPC's were first considered to be very resistant to decay because of the slow moisture transport into the material achieved by at least partial encapsulation of the wood by the polymer matrix (Naghipour 1996). However, it was found that the outermost layer was capable of reaching moisture levels high enough (around 25%) to initiate biological decay (Gnatowski 2009, Wang and Morrell 2004).

Early laboratory and field studies indicated that the wood component in WPC could be susceptible to decay (Clemons and Ibach 2002, Ibach and Clemons 2002, Laks and Verhey 2000, Mankowski and Morrell 2000, Morris and Cooper 1998, Pendelton *et al.* 2002, Verhey *et al.* 2003). In one study, samples of commercial WPC's were exposed for ten years in Hilo, Hawaii (HI), and damage was found to be mainly limited to shallow areas near the surface (Schauwecker *et al*. 2006). Decay fungi fruiting bodies that appear on wood plastic composites have also been described in the past (Manning and Ascherl 2007, Morris and Cooper 1998). However, the mechanism of this process and growth of decay fungal hyphae within the mixture of wood and plastic is not known. Particularly intriguing is the process of destruction by decay fungi of some WPC commercial products exposed to fluctuations in moisture, temperature, ultra violet radiation, as well as biological degradation in outdoor applications.

To support fungal growth, a high moisture content (around 25%), as well as elevated temperature, is required in the WPC wood component as has been demonstrated in the laboratory (Defoirdt *et al.* 2010, Fabiyi *et al.* 2011, Ibach *et al.* 2004, Kim *et al.* 2008, Kim *et al.* 2009; Lomelí-Ramírez *et al.* 2009; Lopez *et al.* 2005; Manning and Ascherl 2007, Segerholm *et al.* 2012, Shirp and Wolcott 2005). The decay process leaves behind damage to the wood component of WPC in the form of cavities or voids left after the wood components (cellulose and/or lignin) have become digested by fungi. Also, mycelia of decay fungi could be observed as a part of this process (Mankowski and Morrell 2000, Ibach *et al.* 2013). Unfortunately, tracking the high moisture level favourable for fungal growth and any internal damage of WPC products, such as in the form of thick boards, is a difficult task. A conventional approach would be cross-sectioning the board of interest and conducting a time consuming and difficult examination of the exposed material in the hope that an area of particular interest would be detected.

This paper presents novel non-destructive approaches for researching the mechanism of internal damage and the assessment of moisture content in WPC with a focus on decay. Large samples of commercial WPC boards exposed in exterior conditions that showed signs of fungal attack were internally examined for the presence of free water by Magnetic Resonance Imaging (MRI), as well as by the micro- and nano-Computed Tomography (CT) scanning techniques. Selected areas of the cross-sectioned surface were also examined using scanning electron microscopy (SEM). Fungal fruiting bodies found on the surface of the exposed boards were further examined.

The MRI technique was demonstrated earlier by the authors of this paper as a non-destructive and effective method for identification of zones containing free water associated with moisture content (MC) above the fiber saturation point in WPC boards (Gnatowski *et al.* 2014). Computer Tomography was recently used for the examination of wood and WPC, providing valuable information about the microstructure of these materials (Cheng *et al.* 2010, Evans *et al.* 2010, Kastner *et al.* 2012). However, in many experiments voxel resolution and limited contrast

between wood components and the plastic matrix was indicated as a limitation of the method (Defoirdt *et al*. 2010). One study used gold-doped plastic in preparing WPC samples to improve CT scan image quality (Wang *et al.* 2007). Our paper presents for the first time the structure of WPC that is being destroyed by decay fungi, including the first reported use of image void analysis to quantitatively analyze the decay process.

2. EXPERIMENTAL METHODS

2.1 Materials

Two types of WPC materials comprising the following formulations were evaluated:

1. Experimental
    a. #106, containing 67.0% pine wood flour
    b. #8, containing 65.9% pine wood flour
2. Commercial
    a. Purchased decking board with two segments tagged #1000 and #1001

Experimental WPCs were formulated based on earlier research and matched the water absorption characteristics (WA) of some commercial WPC decking products available on the North American market around 2002 (Ibach *et al.* 2013, Gnatowski *et al.* 2014). WPC boards were made to match the manufacturing process, dimensions and WA of some selected commercial decking boards. Commercial boards were purchased at a building materials outlet and shipped to an exposure site in Hawaii.

2.2 Samples Exposure, Inspection, and Collection

The experimental #106 board was tagged for identification and then exposed in Vancouver, British Columbia from July 2003 to December 2011. The board was oriented in a horizontal position and fastened using screws in two places to the treated wood frame that was constructed about 305 mm (12”) above the ground. The exposure site was located in shadow under a large Douglas fir tree. Contact with the frame wood was 38 mm (1.5”) wide across the WPC board. Vancouver has an annual average precipitation of 1,118 mm (44”) and an average annual temperature of 11°C (51.8°F) with average minimum around 2°C (35.6°F) and average maximum around 23°C (73.4°F). Just before MR imaging, the board was unscrewed from the frame, the metal identification tag was removed and the board was wrapped tightly in several layers of plastic wrap film. Above freezing temperatures were observed during the period of sample collection. MRI was conducted within a few hours of board removal from the field to avoid drying and water migration.

Two samples of the commercial boards were tagged for identification (#1000 and #1001) and sent to Hilo, Hawaii for outdoor exposure from November 2004 to November 2012. Sample 1000 was exposed in shadow under an Albizia tree while sample 1001 was exposed in an open area under full sunlight. The boards were also exposed in a horizontal position, and fastened with two screws to a frame made from treated wood, similar to how it was done in Vancouver. The boards were installed about 914 mm (36”) above the ground. Hilo has an average annual precipitation of 3200 mm (126”) and average daytime annual temperatures with highs around 27.2°C (80.9°F) and lows around 19.3°C (66.8°F). Both sun and shadow sites were periodically inspected, where the conditions of the boards were documented and samples were collected for evaluation of moisture content and distribution. Samples for this work were collected in November 2012. The samples were marked, carefully wrapped in several layers of plastic wrap film, placed inside a Styrofoam insulated box and couriered overnight to the Polymer Engineering Company (PEC) laboratory. The boards remained wrapped until MRI was conducted two days after their arrival.

Sister samples of both experimental and commercial WPC boards, which had been stored in a warehouse with no contact with exterior conditions, were used for characterization of the different formulations.

2.3 Samples Exposed to Decay Fungi in Laboratory Conditions

Soil block culture testing was conducted according to AWPA E10 (AWPA 2013) on a number of samples consisting of the experimental #8 formulation. Sets of six specimens with dimensions 19 by 19 by 19 mm (3/4 by 3/4 by 3/4 in.) obtained from one strip taken from the board cross-section were used for testing. Since the wood flour in the experimental #8 formulation was pine, the test fungus used was the brown-rot fungus *Gloeophyllum trabeum*, which is known to be more aggressive against softwoods. The test was carried out for 12 weeks. More details regarding samples preparation and exposure to decay are described in an earlier publication (Ibach *et al.* 2013).

2.4 Fungal identification

Fungal fruiting bodies were removed from the boards and dried at 50°C to prevent additional fungal growth. The fruiting bodies were examined by light microscopy at 1000X using Melzer's reagent and KOH/0.5% safranin on an Olympus BX40 microscope and identified using keys and descriptions from Hemmes and Desjardin (2002), and Gilbertson and Ryvarden (1986, 1987).

2.5 Magnetic Resonance Imaging

MRI of the boards was carried out by the Canadian Magnetic Imaging Laboratory in Vancouver, British Columbia. A clinical Siemens Magnetom Espree 1.5 Tesla model TIM [32 x 8] MRI system (Siemens, Germany) was employed. This instrument provided an image zone with field of view (FOV) 320 mm (about 12.6") along the WPC board length. The image matrix 521 x 521 corresponded to the spatial resolution of about 0.55 x 55 mm. For image acquisition, flash gradient echo sequence was employed with an echo time TE of 2.7 ms and repetition time of TR 6.1 ms. MRI scans were performed in three planes shown in Fig. 1. The majority of the scans were performed using the following slicing thickness: Plane 1: 4 mm or 8 mm slicing in a horizontal plane; Plane 2: 8 mm slicing in a vertical plane perpendicular to board length; and Plane 3: 8 mm slicing in a vertical plane parallel to the board length. This selection of slice thickness combined sufficient image detail quality with reasonable imaging time. It was expected that only free water above the fibre saturation point in the wood, which was our primary interest, would be visible on the image in the form of brighter areas due to the relatively long signal lifetime of mobile or free water. The same conditions were used for imaging both experimental and commercial boards.

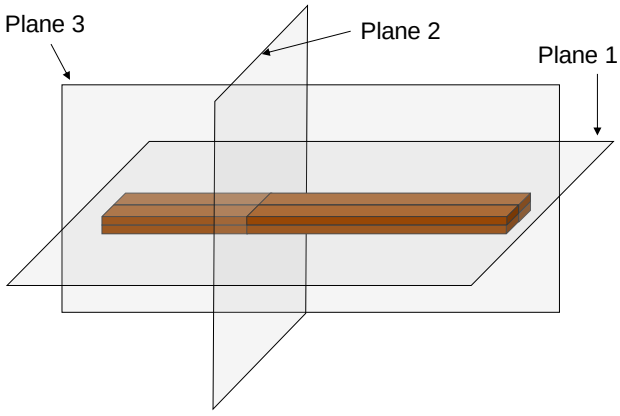

Figure 1: General orientation of the planes in the MRI images; the schematic does not represent the actual location of the planes on the imaged boards

2.6 Micro and Nano X-ray Computed Tomography

X-ray Computed Tomography (CT) was conducted at the GE Inspection Technologies, LP Customer Solutions Center in San Carlos, California. A GE phoenix|x-ray nanotom m (GE Sensing & Inspection Technologies GmbH; Wunstorf, Germany), equipped with a 180 kV high power nanofocus x-ray tube and DXR 500L flat panel detector, was used. This instrument is known for its high scanning resolution (resolving features as small as 200 nm) but also for the high dynamic range of the detector (>10,000:1). This provides high contrast resolution, or the ability to resolve and differentiate between materials of similar densities.

The entire geometry of the samples or selected regions of interest were imaged with 2D acquisition images taken during 360^{o} rotation of the sample. datos|x 2.2 acquisition and reconstruction software (GE Sensing & Inspection Technologies,GmbH; Wunstorf Germany) was used for the acquisition and 3-dimensional (3D) reconstruction of CT images, respectively. VGStudio Max 2.2 (Volume Graphics, GmbH) was used for viewing and analysis of the reconstructed volumes. 2-dimensional (2D) slice images of selected internal cross-sections were obtained.

In addition, for each sample, three sub-volumetric regions with a nominal 50 mm^3 volume were randomly selected for void analysis. The defect detection module in VGStudio Max 2.2 detected the presence, size, and distribution of voids in each selected region and provided the void percentage for each sub-volume. The average void volume for each sample tested was calculated based on the data obtained from the three sub-volumes.

2.6.1 Verification of CT Technique Using Laboratory Decayed Samples

Verification of this technique was first conducted using soil block culture tested samples with known laboratory exposure history and density loss in wood, as well as an unexposed reference sample of the same dimensions. With the known history of the samples, observations could be made to verify and correlate data from CT scans with traditional measures of decay performance of the material.

Decayed sample 8F2 was selected for its relatively high weight loss in wood (28.9%) due to exposure to decay fungi, while sample 8G2 was selected as its counterpart which had undergone the same conditions but was tested without the inoculation of fungi, and had only 4.4% weight loss in wood. Both 8F2 and 8G2 samples were conditioned for 5 days in 70°C water prior to soil block culture testing. A reference untested control sample, 8R2, was also included for comparison purposes. All three samples were sectioned from the same lateral location along the length of the board and are expected to have not only the same composition, but also the most similar microstructure.

CT scans of two soil block culture tested samples, 8F2 and 8G2, along with a reference unexposed sample, 8R2, were collected at 14 µm voxel size and 7.143X magnification. X-ray parameters were standardized for all 3 samples (750 ms timing, 3 averages, 1 skip, 90 kV, 250 µA, and 1100 images). These samples were attached with hot melt glue to thermally stable clear fused quartz rods (Technical Glass Products, Inc.; Painesville, OH) for imaging.

2.6.2 Imaging of Commercial Samples

CT scans were obtained on a reference unexposed board of the sample 1000-1001 material. One end of the 1000 board sample was sectioned, labeled as 1000B, and oriented upright on its longitudinal axis in the nanotom m. The label side was oriented at the top where a 4 cm (1.6”) piece of the material in this region was scanned. The reference sample of the board was scanned using the same orientation. Both the reference 1000-1001 sample and the 1000B cross-section

were CT scanned using a 20 µm voxel size and 5X magnification, x-ray parameters were also standardized (750 ms timing, 3 averages, 1 skip, 90 kV, 300 µA, and 1300 images). Samples were secured to the imaging platform using pressure-sensitive adhesive tape.

2.7 Scanning Electron Microscopy

To evaluate the amount of wood decay, a 3 mm (0.1") thick internal wafer was cut from sample 1000B at the plane from which MRI and CT images was obtained. Samples taken from Area 1 and Area 2, shown in Fig. 7 and 13, were cut in half axially to expose an internal surface for microscopic examination. This sampling method was replicated 4 times each for areas similar in condition to Area 1 and Area 2. Samples were sputter coated with gold in a Denton Desk I vacuum evaporator (Denton Vacuum, Moorestown, NJ) and examined using a Leo Evo 40 electron microscope (Carl Zeiss, NTS, Peabody, Massachusetts).

3. RESULTS AND DISCUSSION

3.1 Inspections of the Commercial Boards

After 28 months of field exposure (in 2007), board 1000 and 1001 showed no obvious signs of fungal growth. Periodical field inspections showed fruiting bodies of decay fungi on WPC boards starting at 40 months of exposure at the sun location. Further inspection a year later showed fruiting bodies on boards exposed in both sun and shadow locations. Additional fruiting bodies were observed with increasing exposure time. . Fig. 2 shows the 1000 and 1001 boards in 2009 (51 months of exposure) with visible fruiting bodies. This was the last inspection of the boards before their collection for evaluation in 2012. Some of the fruiting bodies visible on the surface of the boards after 8 years exposure (November 2012), photographed just before the detailed examinations described in this paper, are shown in Fig. 3 and 4.

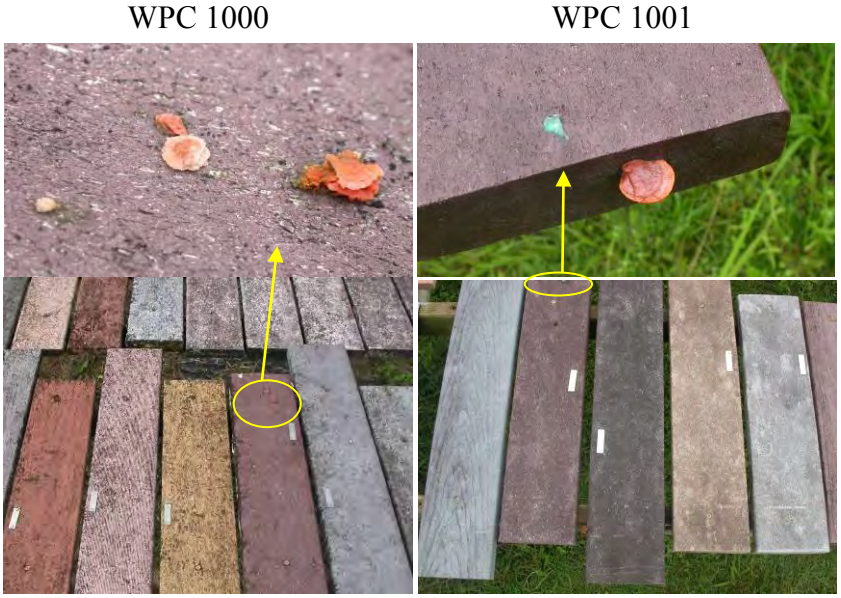

Figure 2: WPC 1000 exposed in shadow location (Left) and 1001 in sun location (Right) in 2009. Areas of interest containing fungi fruiting bodies are marked.

Fig. 3: WPC 1000 after 8 years of shadow exposure, showing (a) top side and (b) bottom side

Fig. 4: WPC 1001 after 8 years of sun exposure, showing (a) top side and (b) bottom side

At least six different species of wood-inhabiting fungi were fruiting on the boards. The bright yellow fruiting bodies, shown in Fig. 3a, are *Dacryopinax spathularia*, a jelly fungus that causes brown-rot. It is a common fungus in Hawaii (Hemmes and Desjardin, 2002) and is frequently associated with plywood, two-by-fours, lanai railings, or any other wood that is wet. The other fungi could not be definitively identified to species due to the lack of basidiospores in the dried specimens. The red fruiting bodies in Fig. 3a and 4a are tentatively identified as the polypore *Pycnoporus sanguineus*, a white rot fungus that is one of the most common shelf polypores in Hawaii (Hemmes and Desjardin, 2002), commonly found on stumps, fallen logs and branches.

The green fruiting body shown in Fig. 4a is most likely a species of the genus *Chlorociboria*, a staining fungus that does not cause significant decay. Other fungi shown in Fig. 3b and 4b may include species within the white-rot genera *Phellinus* and possibly *Ganoderma*; identification to species was not possible due to the extensive degeneration of the old fruiting bodies. Several small, thin fruiting bodies were also observed; these were sterile and could not be identified to genus. The material supports a wide variety of wood-inhabiting fungi, many of which can cause decay.

Moisture content and distribution during the first 51 months of exposure in both sun and shadow locations is shown in Fig. 5. The moisture content and distribution in the graphs indicated relatively moderate water absorption by the boards during this period of time. The MC in wood exceeded 25% only in narrow zones near the board surface in both sun and shadow locations. No catastrophic degradation of the WPC board by fungal decay was expected at this time.

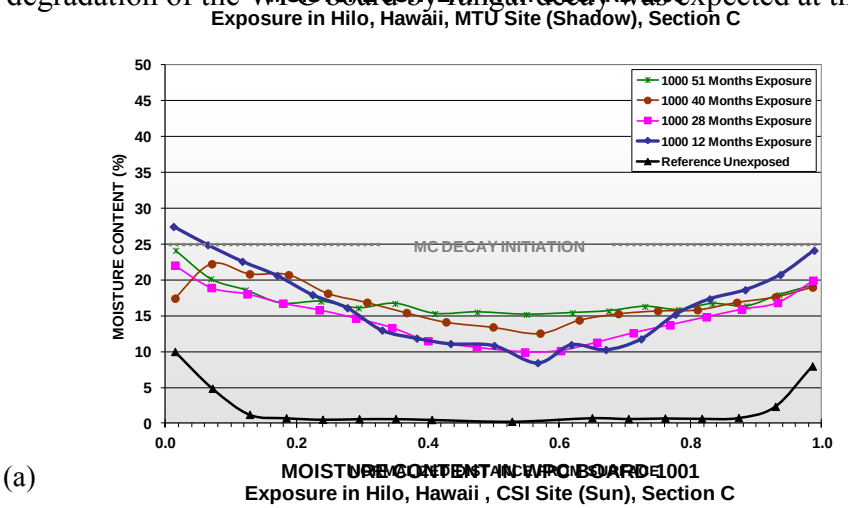

(a)

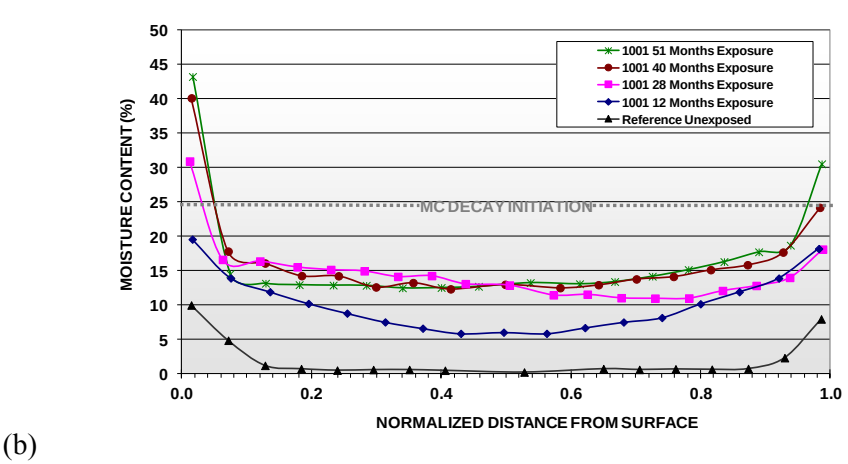

(b)

Figure 5: Moisture content and distribution in the wood component of (a) WPC #1000 exposed in shadow and (b) WPC #1001 exposed in sun, over a 51 month period

3.2 Magnetic Resonance Imaging

3.2.1 Verification of technique used

To verify the free water distribution in the exposed experimental WPC board from MRI imaging, samples were cut, wafered, and dried to measure the WA and MC distribution within the area of interest. The results of this testing are shown in Fig. 6. This figure has been combined with the corresponding segments of MR images to directly compare the bright portion of the image with the water detected in the sample using the destructive testing method.

As shown in Fig. 6, the bright part of the image became gray and began to disappear, matching the black background around the point where the MC in wood reached 22 %. This indicated that the moisture saturation point was most likely reduced in the composite wood flour particles by about 5% as typical fibre saturation occurs for most solid wood species at MC of about 27 to 30%. In general, there is a good correlation between MR images and MC measured by destructive testing involving drying of the samples taken. This experiment confirmed the expectation that free water in WPC could be effectively detected by MRI at a concentration close to fibre saturation or above it using a clinical MRI unit in a non-destructive manner. The MR image shows the border outlining zones of free water presence, i.e. the corresponding potential region of decay activity, and it should be expected that the MC of individual wood particles in these areas may vary to some degree from the 22% detected.

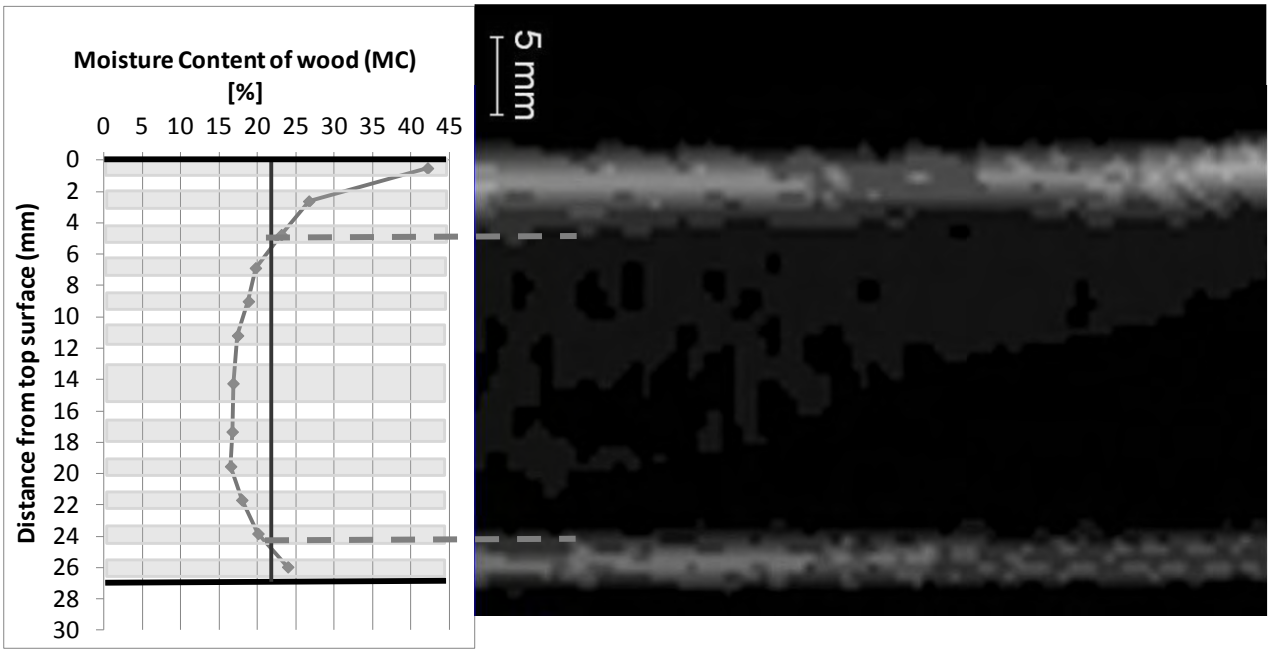

Figure 6: MRI image obtained from plane 2 of experimental WPC #106 showing strong correlation to the moisture content distribution (from destructive testing) throughout the thickness of the imaged region

3.2.2 Imaging of the commercial boards

Non-destructive MR images of the boards showed significant bright areas (spots) visible in the cross-section pictures near the board surface as well as many locations inside the board. In earlier work (Gnatowski *et al* 2014), it was shown that the bright areas indicated the presence of free water in concentrations above the fiber saturation point in the wood flour particles. Selected images of both boards and the location from which they were obtained are shown in Fig. 7. The marked Areas 1 and 2 were later points of focus in the CT and SEM evaluations. The pattern and geometry of areas containing free water are difficult to fully explain at this point and may be attributed to non-uniform wood distribution in the plastic. There is also the strong possibility that the free water detected inside the board was a result of the ongoing decay process. During decay, cellulose of the wood is transformed into CO_2 and H_2O following the reaction (Muller *et al* 2001):

$$C_6H_{12}O_6 + 6O_2 = 6CO_2 + 6H_2O$$

The presence of free water does indicate good conditions for decay fungal growth in these areas. Water generation during the decay process may propagate decay in the WPC due to the entrapment of moisture inside the composite material and its limited water transfer and drying properties. The commercial boards (1000 and 1001) were cut along the MRI slice lines

mentioned above and photographs of the cross-sections are shown in Fig. 8. Wood particles are still well-visible in the cross-sections despite the extensive decay which was later confirmed by SEM and described in Section 3.4.

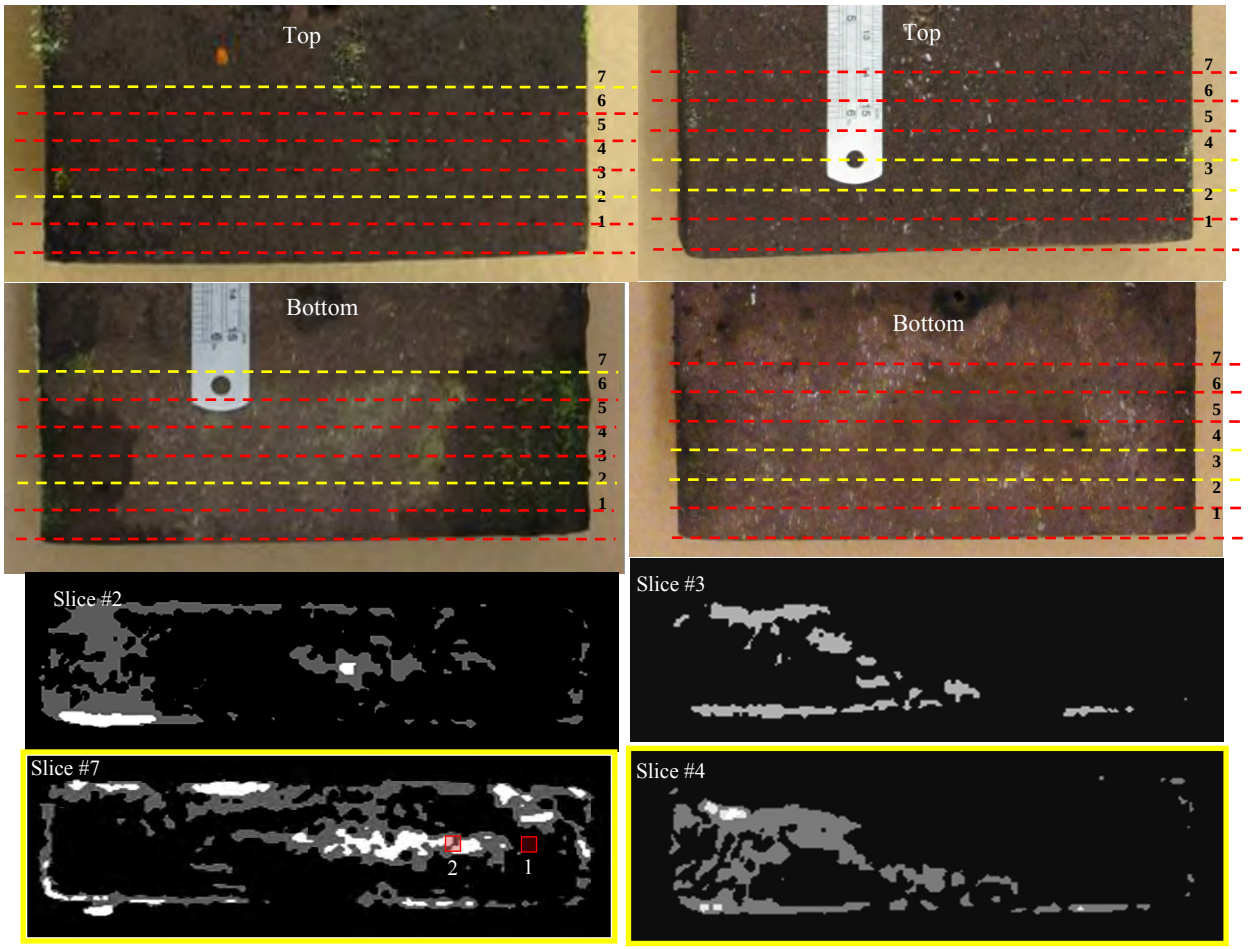

Figure 7: WPC 1000 (left) and 1001(right) imaged by MRI after 8 year of exterior exposure. MRI images of selected cross sections, marked with yellow lines, are presented. Boxed areas 1 and 2 on Slice #7 from WPC 1000 indicate the locations used for subsequent CT and SEM evaluation.

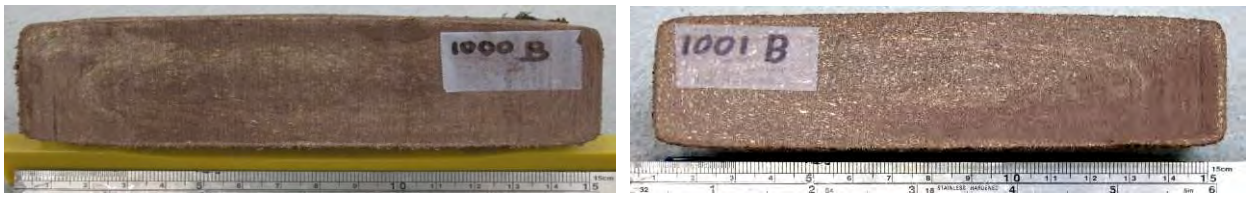

Figure 8: Cross-sections of WPC 1000 corresponding to MRI image slice #4 in Fig. 7 (left) and WPC 1001 corresponding to MRI image slice #7 in Fig. 7 (right)

3.3 Micro X-ray Computed Tomography

3.3.1 Verification of technique used

Fig. 9 to 11 show CT images of 8R2, 8G2, and 8F2 respectively. Fig. 9a, 10a, and 11a show the 3D reconstructed volumes of the samples, annotated with the plane indicating where the subsequent 2D images were obtained. All 2D images were obtained in the extrusion direction and at the center of each sample. Fig. 9c, 10c, and 11c show higher magnification views of the extrusion cross-section of each sample.

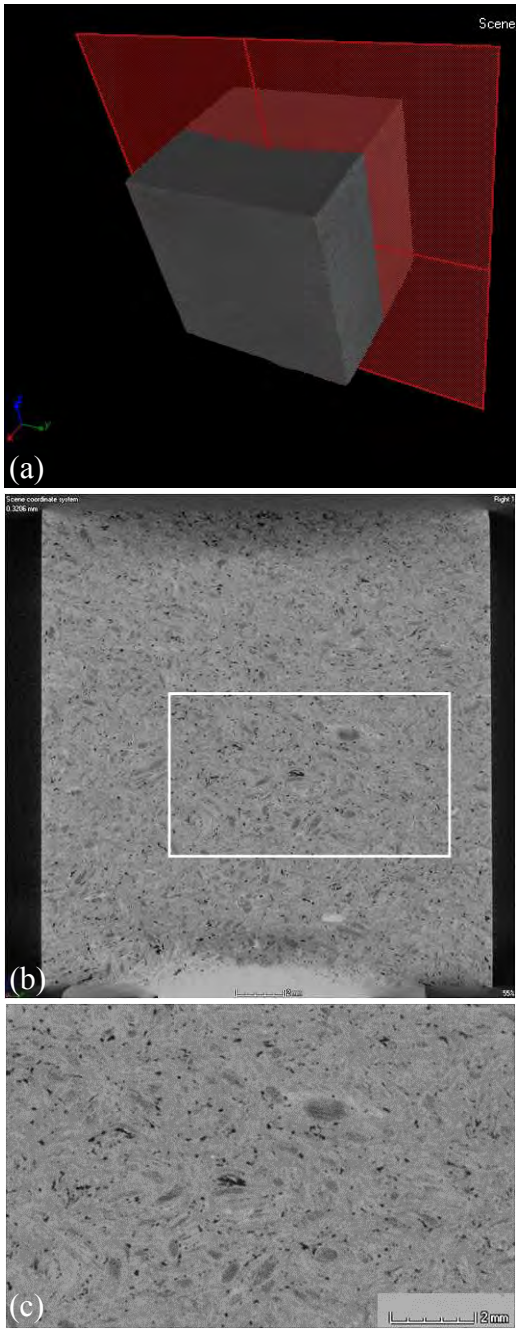

Figure 9: CT images taken in the extrusion direction at the center of the reconstructed volume of experimental reference control sample 8R2 with (a) plane indicator showing where the image was obtained (b) overview image and (c) higher magnification view of voids and wood particles present

Fig. 9c shows that even in the reference material (8R2), there are a number of voids present, as indicated by the darkest areas (of lowest density) on the image. Some individual wood particles can be observed interspersed throughout the polymer matrix; many of these particles appear to be darker grey in colour as compared to the bulk of the material, potentially due to voids that are not filled with resin. Fig. 10c and 11c show the microstructure of samples 8G2 and 8F2 which have both undergone 5 day water immersion at 70°C. It can be seen that microcrack development, in the form of dark outlines, appears to be associated with the pattern of the die used. Sample 8F2 (Fig 11c), which was exposed to fungal decay, shows particularly severe crack development. The structure of the composite, associated with the typical density pattern in relation to the extrusion die used, is well visible on the images.

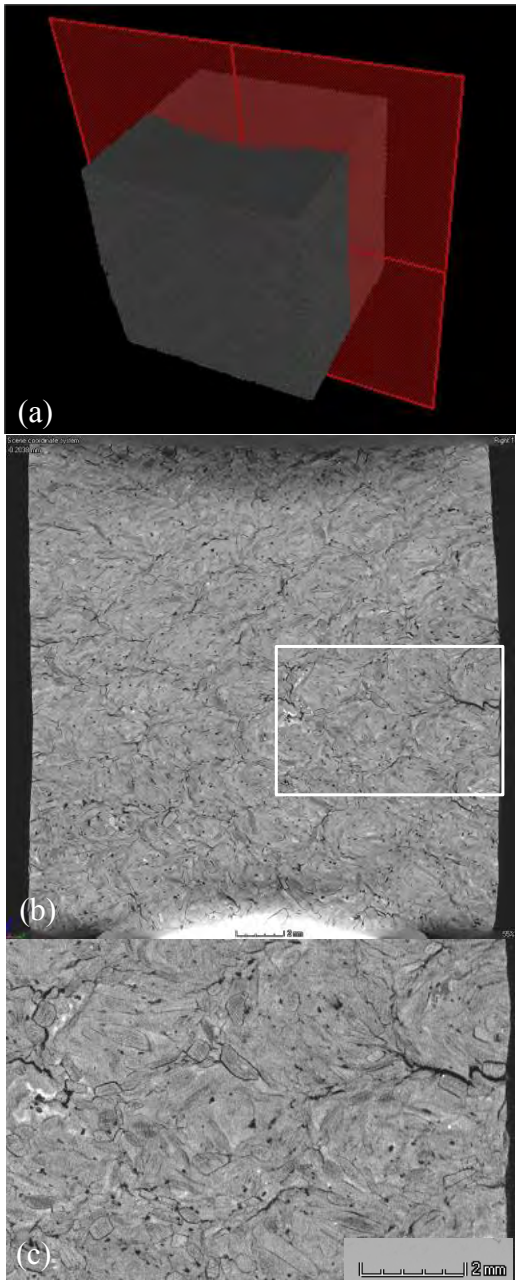

Figure 10: CT images taken in the extrusion direction at the center of the reconstructed volume of experimental conditioned and soil block tested with no fungi sample 8G2 with (a) plane indicator showing where the image was obtained (b) overview image and (c) higher magnification view of microcrack development

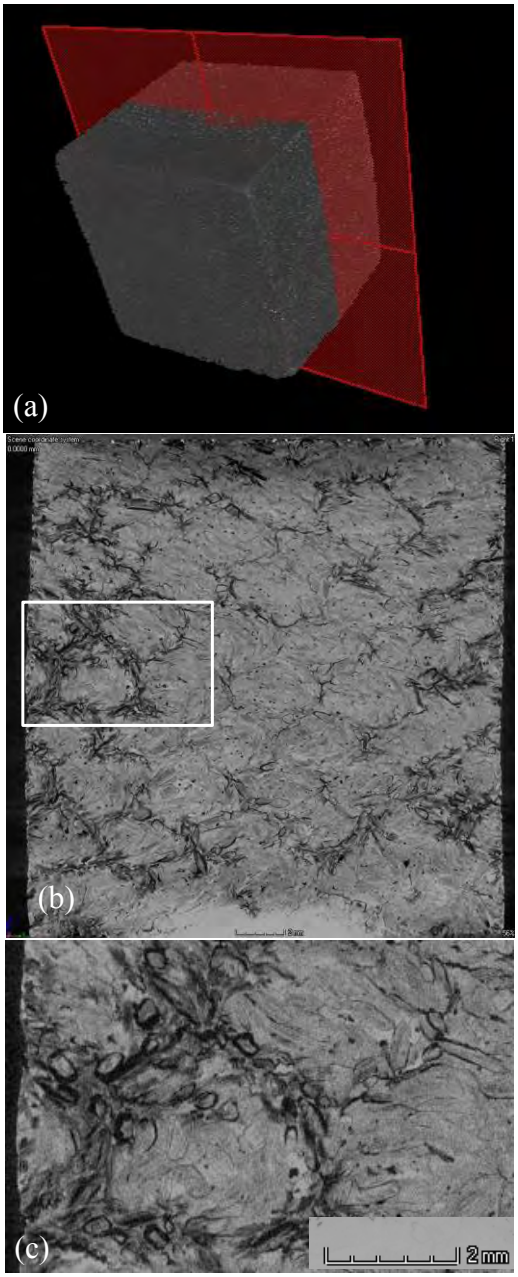

Figure 11: CT images taken in the extrusion direction at the center of the reconstructed volume of experimental conditioned and decayed sample 8F2 with (a) plane indicator showing where the image was obtained (b) overview image and (c) higher magnification view of severe microcrack propagation

As mentioned, voids are present in each of the samples, with the greatest average volume percentage of voids in 8F2 (V_{8F2} = 12.5%), followed by 8G2 (V_{8F2} = 3.8%), and finally 8R2 (V_{8R2} = 1.7%) (Table 1). This trend corresponds well to the weight loss in wood previously found experimentally for the samples, where 28.9% loss had been observed in 8F2 and 4.4% loss was observed for 8G2.

Knowing the voids percentage in samples attributed to wood consumption and leaching during the laboratory exposure and decay process ($V_{8F2} - V_{8R2}$), as well as the theoretical solid wood

density (1.40 g/cm^3), one can calculate the amount of wood loss assuming that all of the voids created during the decay process were once occupied by wood. The wood loss can be divided by the theoretical amount of wood initially present in the WPC based on the initial density of the sample (1.10 g/cm^3) and its known wood content (65.9%). The obtained value of 20.8% wood loss appeared to be a conservative estimate based on the void analysis evaluation, as compared to the percentage wood loss determined experimentally by weighing samples before and after soil block culture testing (28.9%). This difference may be due to certain limitations of the CT method in resolving or detecting voids in the material.

Table 1: Void Analysis Results of Experimental and Commercial WPC Samples

Sample	Exposure Conditions	Void Volume [%]		Detected Volume Ranges [mm^3]
		Average[1]	Standard Deviation[1]	
8R2	Unexposed	1.7	0.5	2.8×10^{-6} - 1.9×10^{-2}
8G2	Lab Conditioned[2]	3.8	1.2	2.8×10^{-6} - 0.81
8F2	Lab Conditioned[2] & Decayed	12.5	1.2	2.8×10^{-6} - 4.9
Ref1000-1001	Unexposed	5.4	4.3	8.0×10^{-6} - 0.52
1000B	Exterior Exposed & Decayed	31.3	4.9	8.0×10^{-6} - 15

[1]Average of three sub-volumes tested
[2]Water immersion for 5 days at 70°C

3.3.2 Imaging of the commercial boards

Fig. 12 and 13 show CT images obtained in the extrusion direction of the unexposed reference 1000-1001sample and the exposed 1000B sample, respectively. Fig. 12a and 13a show the 3D reconstructed volumes of the samples, annotated with the plane indicating where the subsequent 2D images were obtained. Fig. 12c and 13c show higher magnification views of the extrusion cross-section of each sample.

In the reference sample, good distinction of wood particles and voids was achieved. Relatively coarser wood particles and voids were observed (Fig. 12c). The exposed 1000B sample showed a significant number of relatively large dark grey or black areas, most likely voids present in the residual space of decayed wood particles (Fig. 13c). From the greyscale density on the images, it is very difficult to establish an exact decrease in wood density of individual areas of interest, but it could be concluded that the decrease between the reference and exposed commercial samples is significant. The voids seemed to be distributed relatively uniformly across the whole evaluated volume of the exposed 1000B sample, indicating severe and almost complete decay of wood particles.

Void analysis conducted on these samples indicated a great number of voids present in the exposed 1000B cross-section compared to its reference counterpart (Table 1). The average volume percentages of voids for the exposed 1000B sample and the reference 1000-1001 sample were 31.3% and 5.4%, respectively. This indicated that about 25.9% of the voids may have been created by decay process. Based on the initial density of the sample (0.94 g/cm^3) and its known wood content (53%), this would reflect 72.8% wood decay. Density measurements performed on segments of 1000B sample in the area included in the CT scan showed a significant decrease in comparison to the reference material. The exposed 1000B sample and the reference unexposed sample had densities of 0.60 g/cm^3 and 0.94 g/cm^3, respectively, which can be calculated an approximate 68% density loss in wood. This is in relatively good correlation to the wood decay determined by CT void analysis (72.8%). The average 5.4% voids found in the unexposed reference board also explains the relatively low initial density (0.94 g/cm^3) of this board.

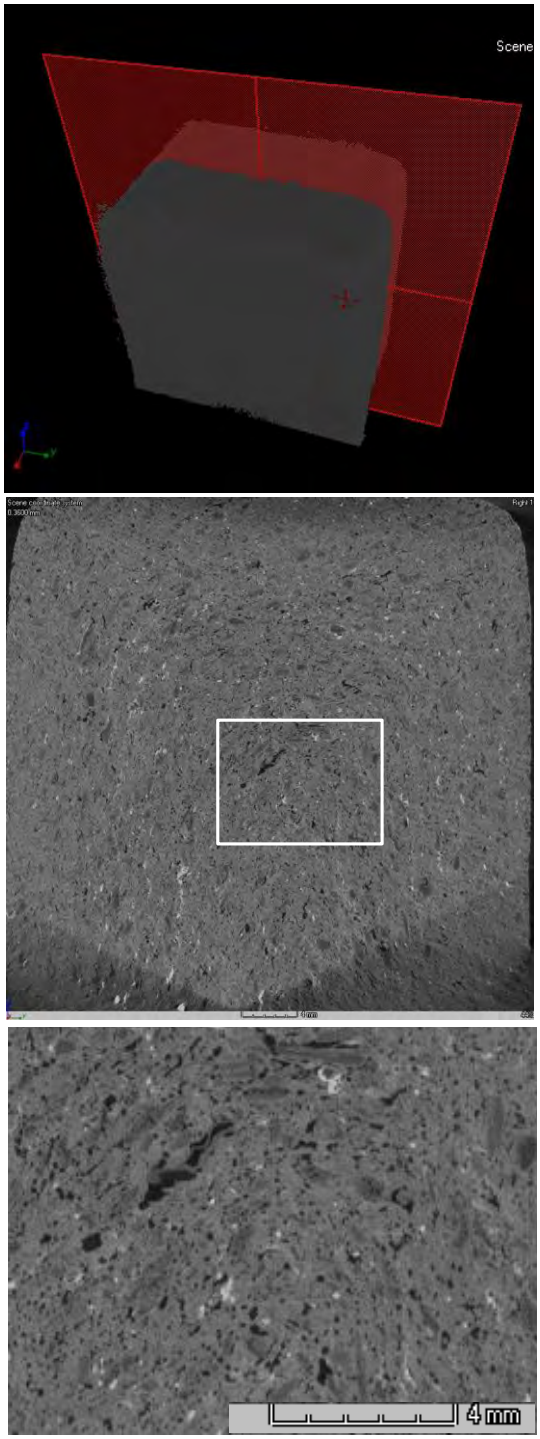

Figure 12: CT images taken in the extrusion direction at the center of the reconstructed volume of commercial reference sample 1000-1001 with (a) plane indicator showing where the image was obtained (b) overview image and (c) higher magnification view of voids and wood particles present

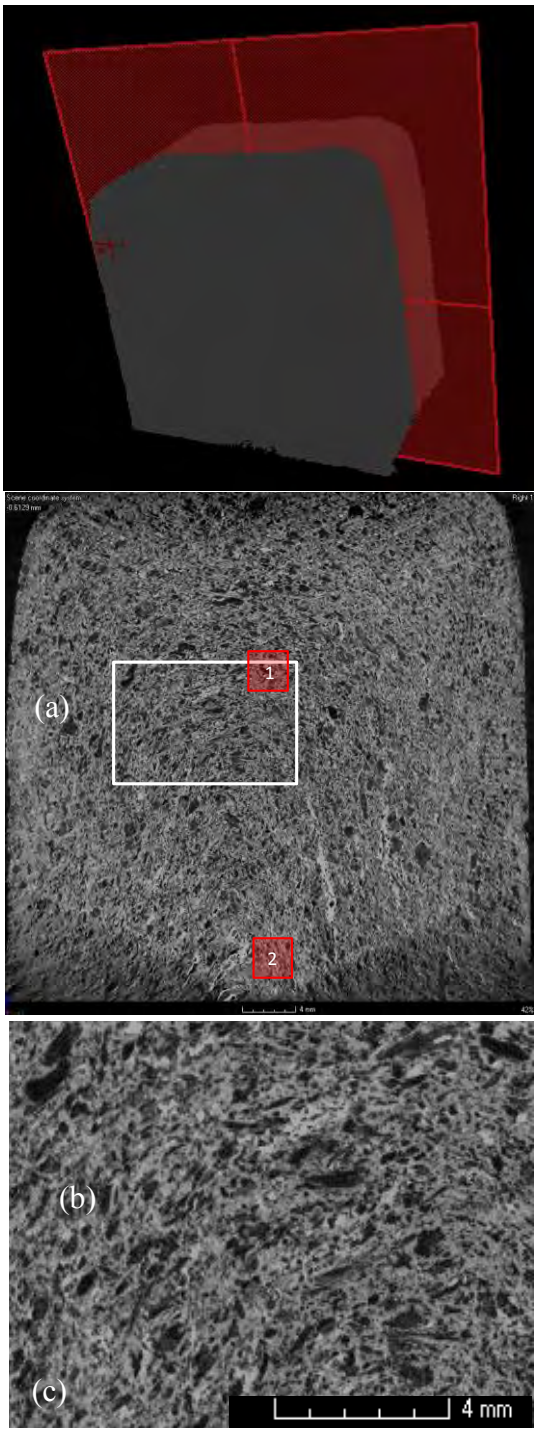

Figure 13: CT images taken in the extrusion direction at the center of the reconstructed volume of commercial exposed sample 1000B with (a) plane indicator showing where the image was obtained (b) overview image and (c) higher magnification view of an abundance of large voids. Boxed Areas 1 and 2 indicate the approximate sub-volume locations for void analysis and correspond to the MR image areas in Fig. 7.

There was no obvious relationship between the free water distribution in the 1000B board as detected by MRI and the average void volume percentage calculated from the CT scan. The calculated void volume content was very similar in two sub-volumes obtained near Areas 1 (28.2%) and 2 (28.7%) indicated in a 2D image of the CT reconstructed volume (Fig. 13b), regardless of the free water absence in Area 1 and its presence in Area 2 shown in the corresponding MR image taken in a similar area (Fig. 7). As mentioned earlier, the presence of free water inside the WPC board may be associated with the decay process still active on the residual wood.

3.4 Scanning Electron Microscopy

Fungi were present on wood pieces in all areas examined throughout the wafer cut from sample 1000B. Many wood pieces were heavily colonized (Fig. 14 and 15). The wood was degraded, with the destruction of the wood symptomatic of a white rot type of decay. Cell walls were thin, and loss of cell wall components caused the S2 layer to pull away from the middle lamella in some cells (Fig. 16). Cell walls were severely degraded in some areas leading to separation of individual wood fibers, loss of cell wall integrity and collapse of wood structure, creating voids occupied by masses of fungal mycelia (Fig. 15). Area 1 and Area 2, as indicated in previous MR (Fig. 7) and CT (Fig. 13) images had similar types and amounts of decay (Fig. 14 and 15), which was confirmed visually in all replicate samples.

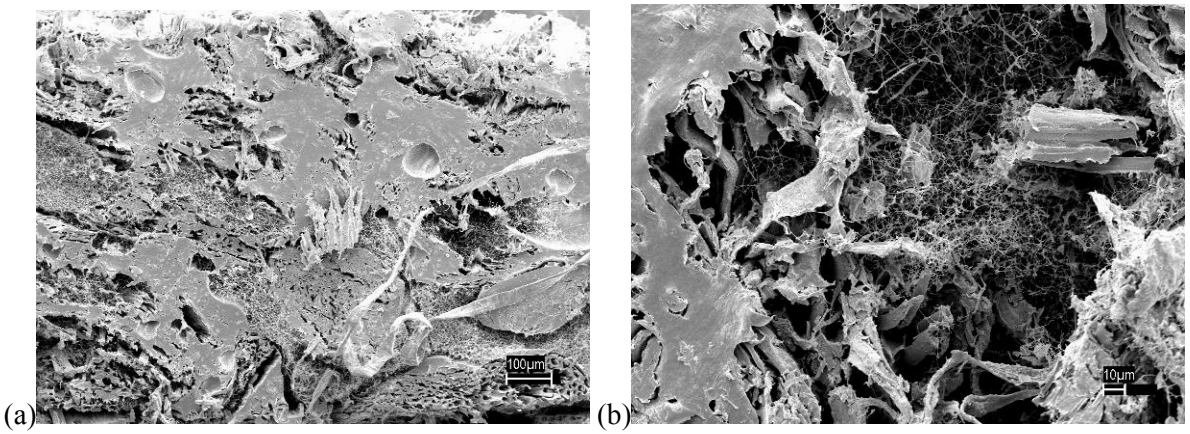

Fig 14: (a) Low and (b) high magnification SEM images of 1000 B, Area 1 with heavy fungal colonization and decay of wood fibers. Area 1 corresponds to the location shown in the MR image in Fig. 7 and the CT image in Fig. 13.

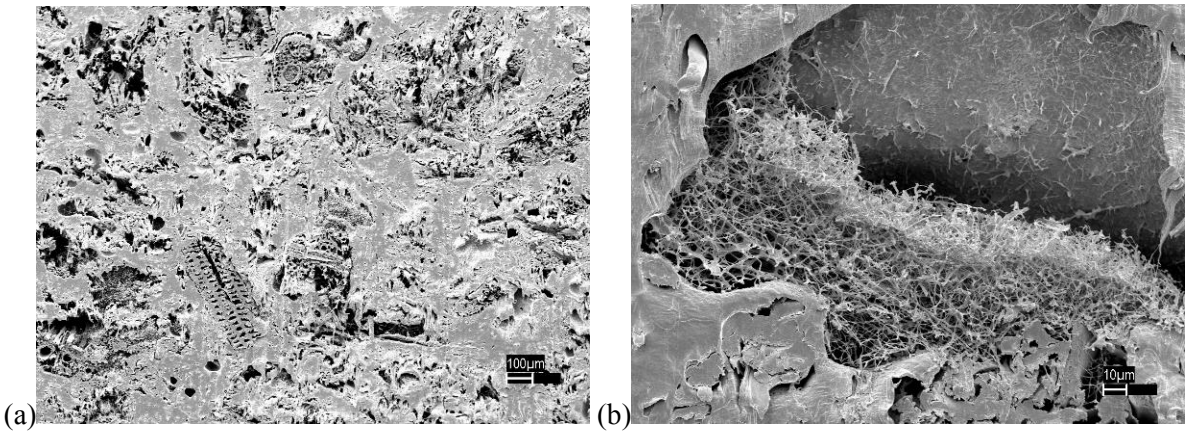

Fig 15: (a) Low and (b) high magnification SEM images of 1000 B, Area 2 showing collapsed wood cells, which left a void occupied by a mycelial mass of wood decay fungi. Area 2 corresponds to the location shown in the MR image in Fig. 7 and the CT image in Fig. 13.

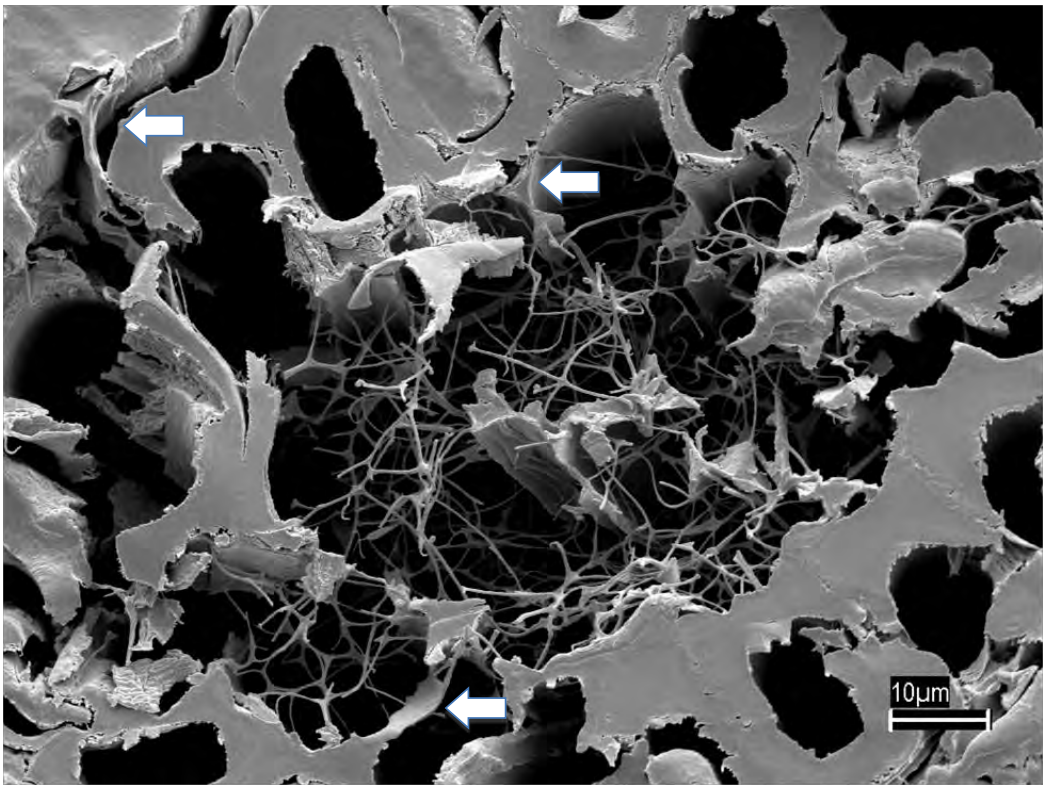

Fig 16: SEM image of 1000 B, Area 2 with symptoms of white rot decay including cell wall thinning, separation of cell wall layers from middle lamella and loss of structural integrity, as indicated by white arrows. Area 2 corresponds to the location shown in the MR image in Fig. 7 and the CT image in Fig. 13.

4. CONCLUSIONS

WPC's can be colonized by a large number of wood fungi species and many of them may decay the wood in the composite. A significant degree of WPC damage by the decay process of the wood was found in the deck boards which were exposed for 8 years in Hawaii. The last field inspection conducted in 2009 indicated relatively moderate water absorption by the boards during approximately 5 years of exposure at both sun and shadow locations and only a limited amount of fungal fruiting bodies were present. Three years later, almost total wood destruction in the WPC (about 70% by weight) was observed, including the center of the boards. The collected data confirmed an earlier observation that the decay process in WPC undergoes an initiation period (Ibach *et al.* 2013). This initiation period depends on the place of exposure and the type of WPC board. The moisture uptake required for the initiation of decay, followed by generation of water inside WPC boards during fungal decomposition of wood, combined with slow water transfer within this material, suggests that the decay process is self-propagating.

MRI was found to be an effective method in the non-destructive detection and evaluation of free water distribution in WPC products, including full cross-sections of decking boards and railings, exposed to exterior conditions. Such detection could be used to warn of favorable conditions for growth of decay fungi. The decay process is always associated with the presence of moisture in wood. In the case of WPC, which has undergone significant decay damage prior to MRI evaluation, moisture may not be visible in the obtained images. This is because empty voids left after the wood decay process may have insufficient retention of free water regardless of advanced decay in the material.

The X-ray CT method was found to be effective in imaging the internal structure of WPC and detecting voids in the composite material, including voids associated with wood decay. Image

analysis of the scans was effective in detection of the areas infected by decay fungi and assessment of the degree of damage. This was verified using laboratory decayed samples with known wood loss and extensive SEM examination of the board samples. Damage to the WPC structure in the form of micro-cracks due to environmental exposure could also be assessed non-destructively using the X-ray CT method. In the heavily damaged WPC samples tested, no correlation was found between the presence of free water and the distribution of voids, or the degree of decay.

Modern instrumental methods are useful in the decay evaluation of WPC's because contrary to solid wood, the decay process in WPC is be difficult to detect. Fungal fruiting bodies do not always develop, even if decay has significantly progressed. Changes in the composite microstructure caused by decay fungi are also not easy to identify during brief field inspections. The testing techniques and equipment presented in this paper are useful in assessing this material for moisture content and distribution as well as environmental and biological degradation.

5. ACKNOWLEDGEMENTS

The authors of this paper would like to thank GE Inspection Technologies, LP for the use of their phoenix|x-ray nanotom m, and Dr. Meghan Faillace, lead applications engineer for GE Inspection Technolgies, LP for her assistance, expertise, and CT imaging of the WPC materials.

6. REFERENCES

American Wood Protection Association (AWPA) (2013): Standard method of testing wood preservatives by laboratory soil-block cultures. AWPA E10. AWPA, Birmingham, Alabama.

ASTM International (2013): ASTM Standard D1037–12, Standard Test Methods for Evaluating Properties of Wood-Base Fiber and Particle Panel Materials. ASTM International, West Conshohocken, Pennsylvania. pp. 31

ASTM International (2013): ASTM Standard D7031–11, Standard Guide for Evaluating Mechanical and Physical Properties of Wood-Plastic Composite Products. ASTM International, West Conshohocken, Pennsylvania. pp. 8

Cheng, Q, Muszynski, L, Shaler, S, Wang, J (2010): Microstructural Changes in Wood Plastic Composites Due to Wetting and Re-drying Evaluated by X-ray Microtomography. *J Nondestruct Eval*. **29**, 207-2013.

Clemons, C M, Ibach, R E (2002): Laboratory tests on fungal resistance of wood filled polyethylene composites. *In*: Proceedings of ANTEC, May 5–9, 2002, San Francisco, California. Society of Plastics Engineers, Newtown, Connecticut. pp. 2219-2222

Defoirdt, N, Gardin, S, Van den Bulcke, J, Van Acker, J (2010): Moisture dynamics of WPC and the impact on fungal testing. *Int. Biodeterior. Biodegrad.* **64**, 65–72.

Evans, P D, Morrison, O, Senden, T J, Vollmer, S, Roberts, R J, Limaye, A, Arns, C H, Averdunk, H, Lowe, A, Knackstedt, M A (2010): Visualization and numerical analysis of adhesive distribution in particleboard using X-ray micro-computed tomography. *International Journal of Adhesion and Adhesives*. **30**, 754-762.

Fabiyi, J S, McDonald, A G, Morrell, J J, Freitag, C (2011): Effects of wood species on durability and chemical changes of fungal decayed wood plastic composites. *Compos. Part A Appl. Sci.Manuf*. **42**, 501–510.

Gilbertson, R.L. and Ryvarden, L. 1986. North American Polypores, Vol 1. Oslo, Norway: Fungiflora. 1-433 pp.

Gilbertson, R.L. and Ryvarden, L. 1987. North American Polypores, Vol 2. Oslo, Norway: Fungiflora. 434-885 pp.

Gnatowski, M (2009): Water Absorption and Durability of Wood-Plastic Composites. In: *Proc. of the 10th International Conf. on Wood & Biofibre Plastic Composites and Cellulose Nanocomposites Symposium*, Madison, WI. pp. 90-102.

Gnatowski, M, Ibach, R E, Leung, M, Sun, G (2014): Magnetic Resonance Imaging Used for the Evaluation of Water Presence in Wood Plastic Composite Boards Exposed to Exterior Conditions. *Wood Material Science and Engineering. In Press*.

Hemmes, D.E. and Desjardin, D.E. 2002. Mushrooms of Hawai'i. Berkely CA: Ten Speed Press. 212 pp.

Ibach, R E, Clemons, C (2002): Biological resistance of polyethylene composites made with chemically modified fibre or flour. In: *6th Pacific Rim Bio-Based Composites Symposium*, ed. P.E. Humphrey, Oregon State University, Portland, Oregon. pp. 574–583.

Ibach, R E, Clemons, C, Stark, N M (2004): Combined ultraviolet and water exposure as a preconditioning method in laboratory fungal durability testing. In: *Seventh International Conference on Woodfiber–Plastic Composites*, ed. N. Stark, May 19–20, 2003, Madison, Wisconsin; Forest Products Society, Madison, Wisconsin. pp. 61–67.

Ibach, R E, Gnatowski, M, Sun, G (2013): Field and Laboratory Decay Evaluations of Wood-Plastic Composites. *Forest Prod. J.* **63**(3/4), 76-87.

Kastner, J, Plank, B, Salaberger, D (2012): High resolution X-ray computed tomography of fibre- and particle-filled polymers. In: *18th World Conference on Nondestructive Testing*. Durban, South Africa, pp. 16-20.

Kim, J W, Harper, D P, Taylor, A M (2008): Effect of wood species on water sorption and durability of wood–plastic composites. *Wood Fiber Sci*. **40**, 519–531.

Kim, J W, Harper D P, Taylor, A M (2009): Effect of extractives on water sorption and durability of wood–plastic composites. *Wood Fiber Sci*. **41**, 279–290.

Laks, P E, Verhey, S A (2000): Decay and termite resistance of thermoplastic/wood fibre composites. In: *Proceedings, 5th Pacific Rim Bio-Based Composites Symposium*, ed. P.D. Evans, Department of Forestry, The Australian National University, Canberra, Australia. pp. 727–734.

Lomelí-Ramírez, M G, Ochoa-Ruiz, H G, Fuentes-Talavera, F J, García-Enriquez, S, Cerpa-Gallegos, M A, Silva-Guzmán, J A (2009): Evaluation of accelerated decay of wood plastic composites by Xylophagus fungi. *Int. Biodeterior. Biodegrad*. **63**, 1030–1035.

Lopez, J L, Cooper, P A, Sain, M, (2005): Evaluation of proposed test methods to determine decay resistance of natural fiber plastic composites. *Forest Prod. J*. **55**, 95–99.

Mankowski, M, Morrell, J J (2000): Patterns of fungal attack in wood–plastic composites following exposure in a soil block test. *Wood Fiber Sci*. **32**, 340–345.

Manning, M J, Ascherl, F (2007): Wood–plastic composite durability and the compelling case for field testing. In: *9th International Conference on Wood & Biofiber–Plastic Composites*, May 21–23, 2007, Madison, Wisconsin; Forest Products Society, Madison, Wisconsin. pp. 217–224.

Morris, P I, Cooper, P (1998): Recycled plastic/wood composite lumber attacked by fungi. *Forest Prod. J*. **48**, 86–88.

Naghipour, B (1996): Effects of extreme environmental conditions and fungal exposure on the properties of wood–plastic composites. Master's thesis. University of Toronto, Ontario, Canada. 70 pp.

Pendleton, D E, Hoffard, T A, Adcock, T, Woodward, B, Wolcott, M P (2002): Durability of an extruded HDPE/wood composite. *Forest Prod. J*. **52**, 21–27.

Schauwecker, C, Morrell, J J, McDonald, A G, Fabiyi, J S, (2006): Degradation of a wood-plastic composite exposed under tropical conditions. *Forest Prod. J.* **56**, 123-129.

Segerholm, B K, Ibach, R W, Walinder, M E P, (2012): Moisture sorption in artificially aged wood–plastic composites. *Bioresources* **7**, 1283–1293.

Shirp, A, Wolcott, M P, (2005): Influence of fungal decay and moisture absorption on mechanical properties of extruded wood–plastic composites. *Wood Fiber Sci*. **37**, 643–652.

Smith, P M, Wolcott, M P (2006): Opportunities for wood/natural fiber–plastic composites in residential and industrial applications. *Forest Prod. J*. **56**, 4–11.

Verhey, S A, Laks, P E, Richter, D L, Keranen, E D, Larkin, G M, (2003): Use of field stakes to evaluate the decay resistance of woodfiber–thermoplastic composites. *Forest Prod. J*. **53**, 67–74.

Wang, W, Morrell, J (2004) Water sorption characteristics of two wood-plastic composites. *Forest Prod. J*. **54** (12), 209-212.